Mono-, Di-, and Trinuclear Complexes Featuring the New Bis(phosphido) Ligand 4,5-Bis(*tert*-butylphosphido)-9,9-dimethylxanthene ([POP]$^{2-}$)

Laura Turculet*,† and Robert McDonald‡

Department of Chemistry, Dalhousie University, Halifax, Nova Scotia, Canada B3H 4J3, and X-Ray Crystallography Laboratory, Department of Chemistry, University of Alberta, Edmonton, Alberta, Canada T6G 2G2

Received August 21, 2007

The synthesis of the new dianionic xanthene-derived bis(phosphido) ligand 4,5-bis(*tert*-butylphosphido)-9,9-dimethylxanthene ([POP]$^{2-}$) is described. Coordination chemistry studies reveal that this versatile new ancillary ligand is capable of supporting electronically and coordinatively unsaturated Zr species (**4**), as well as rationally assembled heteropolynuclear ZrRh (**5**) and $ZrRh_2$ (**6**) complexes.

Introduction

Advances in transition metal-mediated chemistry are largely dependent on the design and synthesis of new types of ancillary ligands that can influence the properties and reactivity of a metal center. In recent years, significant effort has focused on the synthesis of noncyclopentadienyl multidentate ancillary ligands that can provide control over the steric and electronic environment within the metal coordination sphere.[1] Such ligands have traditionally featured both neutral and anionic donor fragments, and while variation of the neutral donors has been explored widely, the anionic donors have largely been restricted to the first-row main group elements C,[2a−c] N,[2d−g] and O.[2h−k]

We are interested in the synthesis and study of complexes supported by new multidentate ancillary ligands featuring formally anionic, heavier main group element donors, in anticipation that such novel ligand architectures will impart unique physical and reactivity properties to the ensuing metal complexes. In this contribution we report the synthesis and preliminary coordination chemistry studies of the new dianionic xanthene-derived bis(phosphido) ligand 4,5-bis(*tert*-butylphosphido)-9,9-dimethylxanthene ([POP]$^{2-}$, Chart 1). Although metal phosphido chemistry is well-precedented across the transition series,[3] relatively little attention has been given to the incorporation of multiple phosphido fragments into the framework of a preformed multidentate ligand.[4,5] Given the utility of Xantphos (Chart 1) and related derivatives in numerous catalytic processes,[6] we considered that the rigid xanthene backbone would provide an effective platform for such dianionic

Chart 1

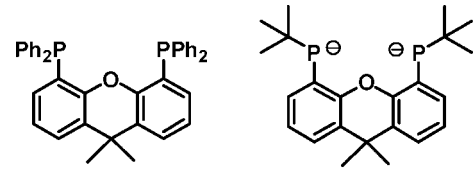

Xantphos [POP]$^{2-}$

* To whom correspondence should be addressed. Fax: 1-902-494-1310. Tel: 1-902-494-6414. E-mail: laura.turculet@dal.ca.

† Dalhousie University.

‡ University of Alberta.

(1) For selected recent reviews see: (a) Piers, W. E.; Emslie, D. J. H. *Coord. Chem. Rev.* **2002**, *131*, 233–234. (b) Bourget-Merle, L.; Lappert, M. F.; Severn, J. R. *Chem. Rev.* **2002**, *102*, 3031. (c) Gibson, V. C.; Spitzmesser, S. K. *Chem. Rev.* **2003**, *103*, 283.

(2) (a) Albrecht, M.; van Koten, G. *Angew. Chem., Int. Ed.* **2001**, *40*, 3750. (b) van der Boom, M. E.; Milstein, D. *Chem. Rev.* **2003**, *103*, 1759. (c) Slagt, M. Q.; van Zwieten, D. A. P.; Moerkerk, A. J. C. M.; Klein Gebbink, R. J. M.; van Koten, G. *Coord. Chem. Rev.* **2004**, *248*, 2275. (d) Kempe, R. *Angew. Chem., Int. Ed.* **2000**, *39*, 468. (e) Gade, L. H. *Chem. Commun.* **2000**, 173. (f) Peters, J. C.; Harkins, S. B.; Brown, S. D.; Day, M. W. *Inorg. Chem.* **2001**, *40*, 5083. (g) Gatard, S.; Celenligil-Cetin, R.; Guo, C.; Foxman, B. M.; Ozerov, O. V. *J. Am. Chem. Soc.* **2006**, *128*, 2808. (h) Bradley, D. C.; Mehrotra, R. C.; Rothwell, I. P.; Singh, A. *Alkoxo and Aryloxo Derivatives of Metals*; Academic Press: San Diego, 2001. (i) Seebach, D.; Beck, A. K.; Heckel, A. *Angew. Chem., Int. Ed.* **2001**, *40*, 92. (j) Brunel, J. M. *Chem. Rev.* **2005**, *105*, 857. (k) Schubert, U. *Acc. Chem. Res.* **2007**, *40*, 730.

(3) For selected examples and reviews, see: (a) Baker, R. T.; Whitney, J. F.; Wreford, S. S. *Organometallics* **1983**, *2*, 1049. (b) Baker, R. T.; Krusic, P. J.; Tulip, T. H.; Calabrese, J. C.; Wreford, S. S. *J. Am. Chem. Soc.* **1983**, *105*, 6763. (c) Chen, H.; Olmstead, M. M.; Pestana, D. C.; Power, P. P *Inorg. Chem.* **1991**, *30*, 1783. (d) Buhro, W. E.; Chisholm, M. H.; Folting, K.; Huffman, J. C.; Martin, J. D.; Streib, W. E. *J. Am. Chem. Soc.* **1992**, *114*, 557. (e) Zwick, B. D.; Dewey, M. A.; Knight, D. A.; Buhro, W. E.; Arif, A. M.; Gladysz, J. A. *Organometallics* **1992**, *11*, 2673. (f) Goel, S. C.; Chiang, M. Y.; Rauscher, D. J.; Buhro, W. E. *J. Am. Chem. Soc.* **1993**, *115*, 160, and references therein. (g) Baker, R. T.; Calabrese, J. C.; Harlow, R. L.; Williams, I. D. *Organometallics* **1993**, *12*, 830. (h) Hey-Hawkins, E. *Chem. Rev.* **1994**, *94*, 1661. (i) Stephan, D. W. *Angew. Chem., Int. Ed.* **2000**, *39*, 314. (j) Urnezius, E.; Klippenstein, S. J.; Protasiewicz, J. D. *Inorg. Chim. Acta* **2000**, *181*, 297. (k) Melenkivitz, R.; Mindiola, D. J.; Hillhouse, G. L. *J. Am. Chem. Soc.* **2002**, *124*, 3846. (l) Scriban, C.; Glueck, D. S.; Di Pasquale, A. G.; Rheingold, A. L. *Organometallics.* **2006**, *25*, 5435. (m) Han, L.-B.; Tilley, T. D. *J. Am. Chem. Soc.* **2006**, *128*, 13698. (n) Derrah, E. J.; Pantazis, D. A.; McDonald, R.; Rosenberg, L. *Organometallics.* **2007**, *26*, 1473, and references therein.

(4) For recent examples of non-cyclopentadienyl mono(phosphido) multidentate ancillary ligands: (a) Izod, K.; Liddle, S. T.; Clegg, W.; Harrington, R. W. *Dalton Trans.* **2006**, 3431. (b) Izod, K.; Liddle, S. T.; Clegg, W. *Chem. Commun.* **2004**, 1748. (c) Izod, K.; Liddle, S. T.; McFarlane, W.; Clegg, W. *Organometallics* **2004**, *23*, 2734, and references therein. (d) Mankad, N. P.; Rivard, E.; Harkins, S. B.; Peters, J. C. *J. Am. Chem. Soc.* **2005**, *127*, 16032. (e) Edwards, P. G.; Parry, J. S.; Read, P. W. *Organometallics* **1995**, *14*, 3649, and references therein. (f) Aspinall, H. C.; Moore, S. R.; Smith, A. K. *J. Chem. Soc., Dalton Trans.* **1993**, 993.

(5) For examples of poly(phosphido) ancillary ligands see: (a) Ellerman, J.; Poersch, P. *Angew. Chem., Int. Ed. Engl.* **1967**, *6*, 355. (b) Bohra, R.; Hitchcock, P. B.; Lappert, M. F.; Leung, W.-P. *J. Chem. Soc., Chem. Commun.* **1989**, 728.

(6) Kamer, P. C. J.; van Leeuwen, P. W. N. M.; Reek, J. N. H. *Acc. Chem. Res.* **2001**, *34*, 895.

10.1021/om700843n CCC: $37.00
Publication on Web 12/05/2007

Scheme 1. Synthesis of $[POP]^{2-}$ and the Mononuclear Zr Complex 4[a]

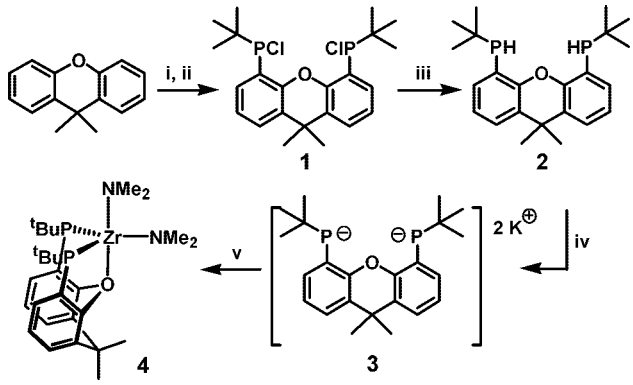

[a] Reagents: (i) 2 *sec*-BuLi, 2 TMEDA; (ii) 2 ^{t}BuPCl$_2$; (iii) LiAlH$_4$; (iv) 2 PhCH$_2$K; (v) Zr(NMe$_2$)$_2$Cl$_2$(DME) (TMEDA = *N*,*N*,*N*′,*N*′-tetramethylethylenediamine; DME = 1,2-dimethoxyethane).

bis(phosphido) ligands. Moreover, while the use of Xantphos and other bis(phosphino)-type ligands is restricted primarily to late transition metal chemistry, we envisioned that dianionic bis(phosphido) ligands would have the potential to support both early and late transition metal centers, as well as multimetallic species. In this context, the design of ancillary ligand architectures that can support multimetallic complexes or metal clusters in a well-defined manner has recently elicited considerable interest, as such assemblies can exhibit physical and/or reactivity properties that are distinct from those of mononuclear species.[7] Herein we report the synthesis and structural characterization of a mononuclear Zr complex featuring $[POP]^{2-}$, as well as di- and trinuclear ZrRh and ZrRh$_2$ derivatives of this new ligand.

Results and Discussion

The $[POP]^{2-}$ ligand was obtained by treatment of 4,5-dilithio-9,9-dimethylxanthene with 2 equiv of ^{t}BuPCl$_2$ to give [POP]Cl$_2$ (**1**) in 74% yield (Scheme 1). Although generation of both *rac*- and *meso*-isomers of **1** is possible, *rac*-**1** is formed almost exclusively in this reaction, as indicated by the presence of a single ^{31}P NMR resonance at 101.5 ppm and a single ^{1}H NMR resonance for the xanthene backbone methyl substituents in the spectra of the crude reaction mixture. In some cases, small amounts of the *meso*-isomer were also detected spectroscopically, but diastereomerically pure *rac*-**1** was readily isolated by crystallization of the crude product. Subsequent reaction of *rac*-**1** with LiAlH$_4$ led to the formation of the secondary phosphine [POP]H$_2$ (**2**) as a mixture of *rac*- and *meso*-isomers (2:3 ratio, as indicated by ^{31}P and ^{1}H NMR spectroscopy) in 81% yield. The phosphine **2** is readily deprotonated with 2 equiv of PhCH$_2$K in THF to give an orange solution of the potassium bis(phosphide) [POP]K$_2$ (**3**). The deprotonation of **2** is quantitative by ^{31}P and ^{1}H NMR spectroscopy, and as such, **3** was most easily generated *in situ* for subsequent reactivity studies. To examine its solid state structure, crystals of **3·OEt$_2$** obtained from diethyl ether solution were examined by use of X-ray diffraction techniques.[8a] The asymmetric unit of the crystallographically determined structure of **3·OEt$_2$** features a P$_2$K$_2$ core in which the phosphide P atoms bridge the potassium cations (Figure 1). Further examination of the unit cell reveals a polymeric structure featuring P···K contacts between adjacent [POP]K$_2$ complexes, as well as contacts between the potassium cations and the aromatic carbons of adjacent [POP]K$_2$ complexes.

Given the established utility of dianionic diamido-type ligands in group 4 transition metal chemistry,[1c,2d] we considered that Zr would provide a reasonable entry point for exploring the coordination chemistry of $[POP]^{2-}$. Toward this end, treatment of **3** with 1 equiv of Zr(NMe$_2$)$_2$Cl$_2$(DME) in THF resulted in formation of the diamido Zr complex [POP]Zr(NMe$_2$)$_2$ (**4**), which was isolated as a red-orange crystalline solid in 53% yield (Scheme 1). The X-ray crystal structure of **4** (Figure 1) confirms the monomeric nature of this complex in the solid state;[8b] the $[POP]^{2-}$ ligand is bound to the metal center in a tridentate fashion, resulting in distorted trigonal bipyramidal geometry at Zr. The xanthene backbone shows significant puckering, with a dihedral angle of 37.41(6)° between the least-squares planes of the aromatic rings. The P atoms in **4** exhibit trigonal-pyramidal geometry ($\Sigma_{\text{angles at P}} = 323°$ (P1), 328° (P2)), thereby rendering each a stereogenic center; in this context the structure of **4** as determined in the course of this crystallographic study corresponds to the *meso*-isomer. The relatively long Zr−P bond lengths in **4** (2.6306(5) and 2.6387(6) Å) are consistent with minimal Zr−P π-interaction[9] and support the description of **4** as being both electronically and coordinatively unsaturated.

In benzene-d_6 solution (300 K), isolated **4** exhibits a single ^{31}P NMR resonance at 71.1 ppm. The ^{31}P NMR spectrum of crude **4** (prior to crystallization) shows no additional resonances that can be attributed to a second diastereomer. The ^{1}H NMR spectrum of **4** (300 K, benzene-d_6) features one resonance at 1.42 ppm for the methyl substituents in the xanthene backbone, as well as only one resonance for the dimethylamido substituents at 2.98 ppm. However, the ^{1}H NMR spectrum of **4** exhibits temperature-dependent line-shape changes, consistent with a nonrigid structure in solution. Most notably, the low-temperature ^{1}H NMR spectrum (203 K, toluene-d_8) features four broad resonances corresponding to the dimethylamido ligands. Line-shape changes are also observed for the methyl substituents in the xanthene backbone and for the *tert*-butyl protons; however, due to the overlapping chemical shifts of these protons, unambiguous assignment of this region of the low-temperature spectrum was not possible. Several dynamic processes can be proposed to account for these temperature-dependent NMR features, including the possibility of slowed (on the

(7) For some recent examples see: (a) Jabri, A.; Korobkov, I.; Gambarotta, S.; Duchateau, R. *Angew. Chem., Int. Ed.* **2007**, *46*, 6119. (b) Keen, A. L.; Doster, M.; Han, H.; Johnson, S. A. *Chem. Commun.* **2006**, 1221. (c) Hatnean, J. A.; Raturi, R.; Lefebvre, J.; Leznoff, D. B.; Lawes, G.; Johnson, S. A. *J. Am. Chem. Soc.* **2006**, *128*, 14992. (d) Anderson, D. J.; McDonald, R.; Cowie, M. *Angew. Chem., Int. Ed.* **2007**, *46*, 3741. (e) Li, H.; Li, L.; Marks, T. J. *Angew. Chem., Int. Ed.* **2004**, *43*, 4937. (f) Harkins, S. B.; Peters, J. C. *J. Am. Chem. Soc.* **2005**, *127*, 2030.

(8) (a) Selected crystal data for **3·OEt$_2$**: monoclinic ($P2_1/c$); a = 12.5425(13) Å; b = 22.708(2) Å; c = 11.3647(12) Å; β = 113.6089(15)°; V = 2965.9(5) Å^3; GOF = 1.022; R_1 = 0.0557; wR_2 = 0.1511. (b) Selected crystal data for **4**: triclinic ($P\bar{1}$); a = 10.2363(12) Å; b = 11.7846(14) Å; c = 12.6010(14) Å; α = 86.3078(14)°; β = 83.1920(14)°; γ = 72.7088(13)°; V = 1440.5(3) Å^3; GOF = 1.058; R_1 = 0.0250; wR_2 = 0.0728. (c) Selected crystal data for **6·OEt$_2$**: monoclinic ($P2_1/c$); a = 20.062(3) Å; b = 12.504(2) Å; c = 21.195(4) Å; β = 110.510(2)°; V = 4980.0(15) Å^3; GOF = 1.034; R_1 = 0.0401; wR_2 = 0.1018.

(9) The range of Zr−P bond lengths for complexes featuring terminal phosphido ligands spans ca. 2.49–2.73 Å; see refs 3a,b and 3h−j herein. For additional discussion on M−P π-interactions see ref 3f cited herein.

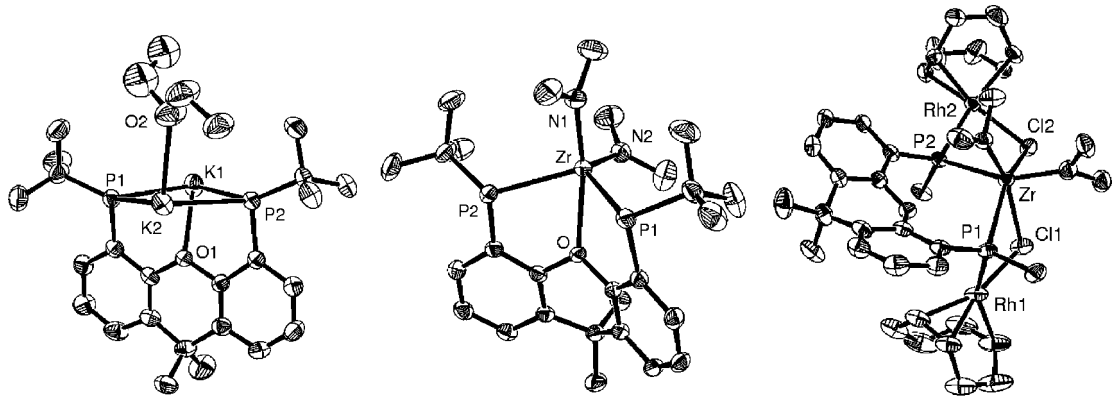

3·OEt₂ **4** **6·OEt₂**

Figure 1. The crystallographically determined structures of **3·OEt₂, 4**, and **6·OEt₂**, shown with 50% displacement ellipsoids. All H atoms, as well as selected C atoms and the diethyl ether solvate in **6·OEt₂**, have been omitted for clarity. Selected interatomic distances (Å) for **3·OEt₂**: K1−P1 3.128(1); K1−P2 3.220(1); K2−P1 3.254(1); K2−P2 3.288(1); K1−O1 2.869(2); K2−O2 2.777(3). Selected interatomic distances (Å) and angles (deg) for **4**: Zr−P1 2.6306(5); Zr−P2 2.6387(6); Zr−O; 2.397(1); Zr−N1 2.024(2); Zr−N2 2.025(2); P1−Zr−P2 107.40(2); O−Zr−N1 163.05(6). Selected interatomic distances (Å) and angles (deg) for **6·OEt₂**: Rh1−P1 2.339(1); Rh2−P2 2.3845(9); Rh1−Cl1 2.410(1); Rh2−Cl2 2.408(1); Zr−P1 2.776(1); Zr−P2 2.792(1); Zr−Cl1 2.681(1); Zr−Cl2 2.674(1); Zr−N1 2.018(3); Zr−N2 2.055(4); P1−Zr−P2 108.70(3).

NMR time scale) inversion at the pyramidal P centers in **4**.[10] However, variable-temperature ^{31}P NMR spectra of **4** do not exhibit decoalescence phenomena at temperatures below 300 K, as would be expected upon slowing of such a dynamic process. Rather, the low-temperature ^{31}P NMR spectra of **4** (233–183 K, toluene-d_8) reveal the presence of a new species in solution, as indicated by the reversible appearance of two new multiplets at 41.8 and 6.2 ppm (1:1 ratio), respectively, in addition to the sharp singlet at 71.1 ppm. It is possible that the new resonances observed at low temperature correspond to diastereomers of **4** that are produced by way of a temperature-dependent equilibrium. We are currently exploring the temperature-dependent solution behavior of **4** in further detail.

Given the established utility of $Cp_2Zr(PR_2)_2$ complexes in the preparation of early late heterobimetallics,[11] we sought to determine if the rigid $[POP]^{2-}$ ligand architecture would support similar multimetallic species. In particular, we wanted to investigate how the potential for electronic and coordinative unsaturation at Zr might influence the properties of the ensuing complexes, as previously reported complexes in which μ-phosphido ligands bridge Zr and a late metal have featured almost exclusively bis(cyclopentadienyl) ligation on Zr. We initially targeted ZrRh complexes, owing to the utility of structurally related bis(phosphino) Rh complexes in catalytic transformations. The reaction of **4** with 0.5 equiv of $[Rh(COD)Cl]_2$ occurred upon mixing the two complexes at room temperature in benzene solution (Scheme 2). The reaction is quantitative on the basis of ^{31}P NMR spectroscopic data, giving rise to the new complex **5**, which at 300 K exhibits two broad ^{31}P NMR resonances at −37.5 and −49.9 (1:1 ratio, benzene, 202.5 MHz). Microcrystalline **5** can be obtained as a red-orange solid in 60% yield by crystallization from pentane. The isolated complex is sparingly soluble in pentane and fully soluble in diethyl ether, benzene, and toluene. In benzene-d_6 solution (300 K), **5** features broad ^{1}H NMR resonances, in addition to broad ^{31}P NMR resonances identical to those observed *in situ*. The low-temperature (253 K, toluene-d_8, 101.3 MHz) ^{31}P NMR spectrum of **5** contains two doublets of doublets (1:1 ratio) centered at −32.4 ($^2J_{PP}$ = 53 Hz, $^1J_{PRh}$ = 91 Hz) and −46.2 ppm ($^2J_{PP}$ = 53 Hz, $^1J_{PRh}$ = 88 Hz), respectively, consistent with a C_1-symmetric structure featuring two magnetically nonequivalent P environments. The low-temperature ^{1}H NMR spectrum is also consistent with such a structure; at 253 K, the ^{1}H NMR spectrum of **5** features four resonances corresponding to the inequivalent vinylic COD protons at 5.25, 4.95, 4.40, and 4.09 ppm, as well as two resonances attributable to the dimethylamido ligands at 3.26 and 2.89 ppm, and two doublets at 1.74 ($^3J_{PH}$ = 13 Hz) and 1.50 ($^3J_{PH}$ = 13 Hz) that correspond to the *tert*-butyl substituents on P. Upon warming to 323 K, complex **5** exhibits additional coalescence phenomena; unfortunately, thermal decomposition of **5** above this temperature precluded a detailed NMR line-shape analysis. We have thus far been unable to obtain X-ray quality crystals of **5**; however, on the basis of these variable-temperature ^{1}H and ^{31}P NMR experiments, as well as its solubility properties, we tentatively assign the structure of **5**

Scheme 2. Synthesis of Dinuclear (5) and Trinuclear (6) Derivatives of $[POP]^{2-}$[a]

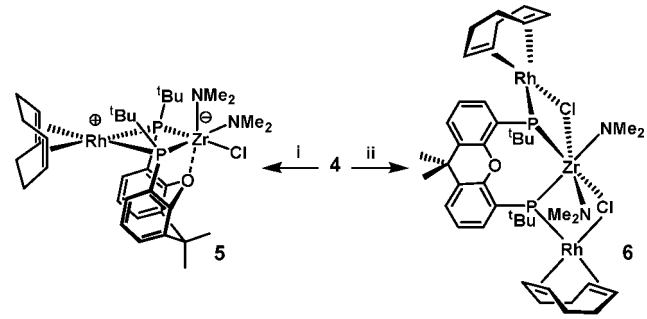

[a] Reagents: (i) 0.5 $[(COD)RhCl]_2$; (ii) $[(COD)RhCl]_2$ (COD = η^4-1,5-cyclooctadiene).

(10) For recent discussions of pyramidal inversion at P in metal phosphido complexes, see: (a) Zhuravel, M. A.; Glueck, D. S.; Zakharov, L. N.; Rheingold, A. L. *Organometallics* **2002**, *21*, 3208, and references therein. (b) Bredeau, S.; Altenhoff, G.; Kunz, K.; Döring S.; Grimme, S.; Kehr, G.; Erker, G. *Organometallics* **2004**, *23*, 1836, and references therein.

(11) (a) Stephan, D. W. *Coord. Chem. Rev.* **1989**, *95*, 41. (b) Wheatley, N.; Kalck, P. *Chem. Rev.* **1999**, *99*, 3379.

as shown in Scheme 2.[12] Although alternative structures for **5** featuring an outer-sphere chloride ion cannot be discounted in the absence of crystallographic evidence, the solubility properties of **5** are consistent with the neutral (zwitterionic) structure depicted in Scheme 2, in which a chloride ion has formally been transferred from Rh to the electronically and coordinatively unsaturated Zr center. This structural proposal is also supported by crystallographic data for the related $ZrRh_2$ trinuclear complex **6**, which reveals the presence of Zr−Cl−Rh bridges (*vide infra*).

In the pursuit of a trinuclear complex supported by $[POP]^{2-}$, treatment of **4** with 1 equiv of $[Rh(COD)Cl]_2$ in benzene solution resulted in an immediate color change from bright yellow to dark red (Scheme 2). The reaction is quantitative by ^{31}P NMR spectroscopy, giving rise to the new complex **6**, which features two sharp doublets (1:1 ratio, benzene) at 2.5 ($^1J_{PRh} = 95$ Hz) and 1.7 ($^1J_{PRh} = 97$ Hz) ppm. The crude product is readily crystallized from diethyl ether at −30 °C to give **6·OEt₂** in 86% yield. The X-ray crystal structure of **6·OEt₂** (Figure 1) confirms the formation of a trinuclear $ZrRh_2$ complex in which both phosphide and chloride ligands bridge Rh and Zr.[8c] As a result, the Zr center is six-coordinate, while each Rh center features the expected square-planar configuration. Notably, the Zr−P bond lengths (2.776(1) and 2.792(1) Å) in **6** are lengthened significantly relative to those of the bis(phosphido) complex **4**, as well as related $Cp_2Zr(\mu\text{-}PR_2)_2RhL_n$ complexes.[12a,b] While early late trinuclear complexes of the type $[Cp_2M'(\mu\text{-}PR_2)_2]_2M$ (e.g., M′ = Zr, Hf; M = Ni, Pd, Pt) are known,[13] **6** represents the first trinuclear complex of this type to feature two late transition metal centers in a M−P−Zr−P−M motif. Unlike **4** and **5**, isolated **6** exhibits ^{31}P NMR features (benzene-d_6) identical to those observed *in situ*, with no apparent temperature dependence; the ^1H and ^{13}C NMR spectra of **6** (300 K, benzene-d_6) are also consistent with the C_1-symmetry observed in the solid state.

Conclusions

In summary, the synthesis and preliminary coordination chemistry of the new xanthene-derived bis(phosphido) ancillary ligand ($[POP]^{2-}$) have been reported herein. This versatile new ancillary ligand has proven capable of supporting electronically and coordinatively unsaturated Zr species, as well as rationally assembled heteropolynuclear ZrRh and $ZrRh_2$ complexes. Encouraged by these preliminary findings, we are currently exploring the physical and reactivity properties of a wider range of main group and transition metal derivatives of $[POP]^{2-}$ and related phosphido-based multidentate ancillary ligands. Results of these synthetic and reactivity studies will be reported in due course.

Experimental Section

General Considerations. All experiments were conducted under nitrogen in an MBraun glovebox or using standard Schlenk techniques. Dry, oxygen-free solvents were used unless otherwise indicated. All nondeuterated solvents were deoxygenated and dried by sparging with nitrogen and subsequent passage through a double-column solvent purification system provided by MBraun Inc. Tetrahydrofuran and diethyl ether were purified over two activated alumina columns, while benzene, toluene, and pentane were purified over one activated alumina column and one column packed with activated Q-5. All purified solvents were stored over 4 Å molecular sieves. Distilled water was deoxygenated by sparging with nitrogen for ca. 40 min. Benzene-d_6, tetrahydrofuran-d_8, and toluene-d_8 were degassed via three freeze–pump–thaw cycles and stored over 4 Å molecular sieves. ^1H, ^{13}C, and ^{31}P NMR characterization data were collected at 300 K on a Bruker AV-500 spectrometer operating at 500.1, 125.8, and 202.5 MHz (respectively) with chemical shifts reported in parts per million downfield of $SiMe_4$ (for ^1H and ^{13}C) or 85% H_3PO_4 in D_2O (for ^{31}P). Variable-temperature NMR data were collected on a Bruker AC-250 spectrometer. ^1H and ^{13}C NMR chemical shift assignments are based on data obtained from ^{13}C-DEPT, $^1H-^1H$ COSY, $^1H-^{13}C$ HSQC, and $^1H-^{13}C$ HMBC NMR experiments. In some cases, fewer than expected unique ^{13}C NMR resonances were observed, despite prolonged acquisition times. Elemental analyses were performed by Desert Analytics, Inc. of Tucson, AZ, and Canadian Microanalytical Service Ltd. of Delta, British Columbia, Canada. $[Rh(COD)Cl]_2$ (COD = η^4-1,5-cyclooctadiene) was purchased from Strem and used as received. The compounds $PhCH_2K$[14] and $Zr(NMe_2)_2Cl_2(DME)$[15] (DME = 1,2-dimethoxyethane) were prepared according to literature procedures. Unless otherwise specified, all other reagents were purchased from Aldrich and used without further purification.

***rac*-9,9-Dimethyl-4,5-di(*tert*-butylchlorophosphino)xanthene (*rac*-[POP]Cl₂, *rac*-1).** A solution of *sec*-butyllithium in cyclohexane (13.6 mL, 19.0 mmol, 1.4 M) was added slowly via syringe to a room-temperature solution of 9,9-dimethylxanthene (2.0 g, 9.5 mmol) and TMEDA (2.87 mL, 19.0 mmol) in ca. 100 mL of diethyl ether. The resulting red-brown reaction mixture was allowed to stir at room temperature for 20 h, after which time the mixture was cooled to −78 °C. To this mixture was added dropwise a precooled (−78 °C) solution of $^tBuPCl_2$ (3.0 g, 19.0 mmol) in ca. 100 mL of diethyl ether. The resulting reaction mixture was allowed to warm to room temperature and stir for an additional 16 h. Subsequently, the volatile components were removed *in vacuo* and ca. 150 mL of pentane was added to the residue. The pentane solution was filtered to remove an off-white precipitate, and the filtrate was evaporated to dryness, affording crude *rac*-**1** as a white solid. In some instances, *meso*-**1** was also observed as a minor isomer. Crystallization from pentane at −30 °C gave isomerically pure *rac*-**1** as a white crystalline solid (3.2 g, 74%). ^1H NMR (500 MHz, benzene-d_6): δ 7.76 (m, 2 H, H_{arom}), 7.07 (m, 2 H, H_{arom}), 6.90 (m, 2 H, H_{arom}), 1.31 (s, 6 H, CMe_2), 1.17 (m, 18 H, PCMe_3). $^{13}C\{^1H\}$ NMR (125.8 MHz, benzene-d_6): δ 152.1 (m, *C*O), 132.2 (*C*H$_{arom}$), 129.8 (*C*CMe$_2$), 128.9 (*C*H$_{arom}$), 124.9 (d, *C*PCMe$_3$, $^1J_{CP} = 50$ Hz), 124.0 (*C*H$_{arom}$), 36.6 (m, P*C*Me$_3$), 34.5 (*C*Me$_2$), 33.1 (C*Me*$_2$), 26.1 (m, PC*Me*$_3$). $^{31}P\{^1H\}$ NMR (202.5 MHz, benzene-d_6): δ 101.5. Anal. Calcd for $C_{23}H_{30}Cl_2OP_2$: C, 60.67; H, 6.64. Found: C, 60.67; H, 6.75.

9,9-Dimethyl-4,5-di(*tert*-butylphosphino)xanthene ([POP]H₂, 2). A solution of *rac*-**1** (3.2 g, 7.0 mmol) in ca. 100 mL of diethyl ether was added dropwise via cannula to a cold (−78 °C) solution of $LiAlH_4$ (0.27 g, 7.0 mmol) in 50 mL of diethyl ether, resulting in a white precipitate. The reaction mixture was allowed to warm to room temperature and stir for an additional 4 h. The mixture was then cooled to 0 °C, and the reaction was quenched by dropwise addition of 20 mL of degassed water. The organic fraction was cannula transferred away from the aqueous layer, which was extracted with diethyl ether (2 × 50 mL). All organic fractions were combined and dried over anhydrous $MgSO_4$ under a nitrogen atmosphere. Following filtration, the volatile components were

(12) Structurally related ZrRh heterometallic complexes of the type $Cp_2Zr(\mu\text{-}PR_2)RhL_n$ have been reported: (a) Baker, R. T.; Tulip, T. H. *Organometallics* **1986**, *5*, 839. (b) Gelmini, L.; Stephan, D. W. *Organometallics* **1988**, *7*, 849. (c) Larsonneur, A.-M.; Choukroun, R.; Daran, J.-C.; Cuenca, T.; Flores, J. C.; Royo, P. *J. Organomet. Chem.* **1993**, *83*, 444.

(13) Baker, R. T.; Fultz, W. C.; Marder, T. B.; Williams, I. D. *Organometallics* **1990**, *9*, 2357.

(14) Schlosser, M.; Hartmann, J. *Angew. Chem., Int. Ed. Engl.* **1973**, *12*, 508.

(15) Warren, T. H.; Erker, G.; Fröhlich, R.; Wibbeling, B. *Organometallics* **2000**, *19*, 127.

removed *in vacuo*, affording a mixture of *rac*- and *meso*-**2** (2:3 ratio) as a viscous, colorless oil that solidified upon standing (2.2 g, 81%). ^{1}H NMR (500 MHz, benzene-d_6) *rac*-**2**: δ 7.33 (m, 2 H, H_{arom}), 7.13 (m, 2 H, H_{arom}), 6.88 (m, 2 H, H_{arom}), 4.63 (d, 2 H, P*H*, $^1J_{PH}$ = 211 Hz), 1.37 (s, 6 H, CMe_2), 1.23 (d, 18 H, PCMe_3, $^3J_{PH}$ = 12 Hz); *meso*-**2**: δ 7.33 (m, 2 H, H_{arom}), 7.13 (m, 2 H, H_{arom}), 6.88 (m, 2 H, H_{arom}), 5.81 (d, 2 H, P*H*, $^1J_{PH}$ = 214 Hz), 1.42 (s, 3 H, CMe_2), 1.33 (s, 3 H, CMe_2), 1.21 (d, 18 H, PCMe_3, $^3J_{PH}$ = 12 Hz). ^{13}C{^{1}H} NMR (125.8 MHz, benzene-d_6): δ 153.9 (*C*O, *rac*-**2**), 153.1 (*C*O, *meso*-**2**), 137.0 (m, *C*H$_{arom}$), 136.7 (m, *C*H$_{arom}$), 131.2 (*C*CMe$_2$, *rac*-**2**), 131.0 (*C*CMe$_2$, *meso*-**2**), 127.3 (*C*H$_{arom}$), 127.2 (*C*H$_{arom}$), 123.9 (*C*PCMe$_3$, *meso*- and/or *rac*-**2**), 123.6 (*C*H$_{arom}$), 35.3 (*C*Me$_2$, *meso*-**2**), 35.2 (*C*Me$_2$, *rac*-**2**), 33.3 (C*Me*$_2$, *meso*-**2**), 31.8 (C*Me*$_2$, *rac*-**2**), 30.7 (C*Me*$_2$, *meso*-**2**), 31.0–30.6 (PC*Me*$_3$, P*C*Me$_3$). ^{31}P NMR (202.5 MHz, benzene-d_6): δ −30.0 (d, *rac*-**2**, $^1J_{PH}$ = 216 Hz), −33.2 (d, *meso*-**2**, $^1J_{PH}$ = 216 Hz). Anal. Calcd for $C_{23}H_{32}OP_2$: C, 71.48; H, 8.35. Found: C, 71.49; H, 8.71.

Generation of [POP]K$_2$ (3). A solution of PhCH$_2$K (0.12 g, 0.88 mmol) in 5 mL of THF was added to a cold (−30 °C) solution of **2** (0.17 g, 0.44 mmol) in 5 mL of THF. The resulting orange solution was allowed to warm to room temperature and stir for an additional 30 min. ^{31}P NMR analysis of the reaction mixture at this stage indicated quantitative conversion to **3**. The volatile components were removed *in vacuo*, affording **3·(THF)$_x$** as a yellow-orange solid, which was characterized spectroscopically. Given the quantitative nature of this reaction and the variable amount of coordinated THF (x) in the isolated product, **3** was most easily generated *in situ* for subsequent reactivity studies. ^{1}H NMR (500 MHz, THF-d_8): δ 7.03 (m, 2 H, H_{arom}), 6.49 (m, 2 H, H_{arom}), 6.25 (m, 2 H, H_{arom}), 1.46 (s, 6 H, CMe_2), 1.39 (m, 18 H, PCMe_3). ^{13}C{^{1}H} NMR (125.8 MHz, THF-d_8): δ 152.7 (d, *C*PCMe$_3$, $^1J_{CP}$ = 75 Hz), 146.8 (m, *C*O), 127.4 (*C*CMe$_2$), 125.7 (*C*H$_{arom}$), 122.4 (*C*H$_{arom}$), 111.0 (*C*H$_{arom}$), 34.6 (*C*Me$_2$), 34.0 (m, PCMe_3), 33.6 (CMe_2), 28.9 (m, P*C*Me$_3$). ^{31}P{^{1}H} NMR (202.5 MHz, THF-d_8): δ 3.7. A single crystal of **3·OEt$_2$** suitable for X-ray diffraction analysis was grown from diethyl ether at −30 °C.

[POP]Zr(NMe$_2$)$_2$ (4). A solution of **3** in THF (50 mL) generated from **2** (1.00 g, 2.59 mmol) and PhCH$_2$K (0.67 g, 5.18 mmol) was cooled to −30 °C and added dropwise to a stirred solution of ZrCl$_2$(NMe$_2$)(DME) (0.89 g, 2.59 mmol) in 20 mL of THF. The resulting dark red reaction mixture was allowed to stir for 30 min at room temperature. The volatile components were removed *in vacuo*, and the remaining orange residue was extracted into ca. 75 mL of pentane. The pentane extracts were filtered through Celite, concentrated to ca. 50 mL volume, and refrigerated at −30 °C to give **4** as a yellow-orange crystalline solid (0.77 g, 53%). ^{1}H NMR (500 MHz, benzene-d_6): δ 7.58 (m, 2 H, H_{arom}), 6.97 (m, 2 H, H_{arom}), 6.87 (m, 2 H, H_{arom}), 2.98 (s, 12 H, NMe_2), 1.53 (d, 18 H, PCMe_3, $^3J_{PH}$ = 13 Hz), 1.42 (s, 6 H, CMe_2). ^{13}C{^{1}H} NMR (125.8 MHz, benzene-d_6): δ 153.9 (m, *C*O), 133.8 (d, *C*PCMe$_3$, $^1J_{CP}$ = 36 Hz), 131.2 (*C*H$_{arom}$), 131.0 (*C*CMe$_2$), 124.7 (*C*H$_{arom}$), 120.3 (*C*H$_{arom}$), 40.6 (N*Me*$_2$), 35.6 (d, P*C*Me$_3$, $^1J_{CP}$ = 18 Hz), 34.4 (m, *C*Me$_2$), 33.2 (m, PCMe_3), 30.5 (CMe_2). ^{31}P{^{1}H} NMR (202.5 MHz, benzene-d_6): δ 71.1. Anal. Calcd for $C_{27}H_{42}N_2OP_2Zr$: C, 57.52; H, 7.51; N, 4.97. Found: C, 57.75; H, 7.42; N, 4.86. A single crystal of **4** suitable for X-ray diffraction analysis was grown from pentane at −30 °C.

[POP]Zr(NMe$_2$)$_2$·Rh(COD)Cl (5). A solution of **4** (0.15 g, 0.27 mmol) in 5 mL of benzene was added to a slurry of [Rh(COD)Cl]$_2$ (0.07 g, 0.13 mmol) in 2 mL of benzene at room temperature. The resulting dark red reaction mixture was allowed to stir for 30 min at room temperature. The volatile components were then removed under vacuum, and the residue was extracted into ca. 20 mL of pentane. The pentane solution was refrigerated at −30 °C to give **5** as red-orange microcrystals (0.13 g, 60%). ^{1}H NMR (500 MHz, benzene-d_6): δ 7.52 (br s, 2 H, H_{arom}), 6.98 (m, 2 H, H_{arom}), 6.91 (m, 2 H, H_{arom}), 5.10 (br s, 2 H, COD), 4.27 (br s, 2 H, COD), 3.09 (br s, 12 H, NMe_2), 2.07 (br s, 2 H, COD), 1.63 (s, 3 H, CMe_2), 1.62 (br s, 18 H, PCMe_3), 1.50 (s, 3 H, CMe_2), 1.19 (br m, 4 H, COD), 1.00 (br s, 2 H, COD). ^{13}C{^{1}H} NMR (125.8 MHz, benzene-d_6): δ 155.6 (*C*O), 136.0 (*C*CMe$_2$), 128.2 (*C*H$_{arom}$), 126.0 (*C*H$_{arom}$), 120.4 (*C*H$_{arom}$), 86.0 (COD), 82.9 (COD), 43.8 (N*Me*$_2$), 37.7 (*C*Me$_2$), 33.3 (br, PCMe_3), 31.8 (br, COD), 30.5 (br, COD), 29.5 (CMe_2), 22.9 (CMe_2). ^{31}P{^{1}H} NMR (202.5 MHz, benzene-d_6): δ −37.5 (br, 1 P, Rh-*P*-Zr), −49.6 (br, 1 P, Rh-*P*-Zr). ^{31}P{^{1}H} NMR (101.3 MHz, 253 K, toluene-d_8): δ −32.4 (dd, 1 P, Rh-*P*-Zr, $^2J_{PP}$ = 53 Hz, $^1J_{PRh}$ = 91 Hz), −46.2 (dd, 1 P, Rh-*P*-Zr, $^2J_{PP}$ = 53 Hz, $^1J_{PRh}$ = 88 Hz). Anal. Calcd for $C_{35}H_{54}ClN_2OP_2RhZr$: C, 51.88; H, 6.72; N, 3.46. Found: C, 51.59; H, 6.42; N, 3.44.

{[POP]Zr(NMe$_2$)$_2$·[Rh(COD)Cl]$_2$}OEt$_2$ (6·OEt$_2$). A solution of **4** (0.07 g, 0.12 mmol) in 5 mL of benzene was added to a slurry of [Rh(COD)Cl]$_2$ (0.06 g, 0.12 mmol) in 2 mL of benzene at room temperature. The resulting dark red reaction mixture was allowed to stir for 30 min at room temperature. The volatile components were then removed under vacuum, and the residue was extracted into ca. 15 mL of diethyl ether. The ether extracts were filtered through Celite, concentrated to ca. 7 mL volume, and refrigerated at −30 °C to give **6·OEt$_2$** as a yellow crystalline solid (0.12 g, 86%). Crystallographic studies confirm that the diethyl ether solvate in **6·OEt$_2$** is not within the coordination sphere of Zr or Rh. ^{1}H NMR (500 MHz, benzene-d_6): δ 7.80 (m, 1 H, H_{arom}), 7.53 (br m, 1 H, H_{arom}), 7.20 (m, 1 H, H_{arom}), 7.09 (m, 1 H, H_{arom}), 6.94 (m, 2 H, H_{arom}), 5.08 (br m, 2 H, COD), 5.04 (br m, 2 H, COD), 4.37 (br m, 2 H, COD), 4.30 (br m, 2 H, COD), 3.37 (s, 6 H, NMe_2), 3.26 (q, 4 H, OCH_2CH$_3$, $^3J_{HH}$ = 7 Hz) 2.96 (s, 6 H, NMe_2), 2.35 – 2.18 (br m, 4 H, COD), 2.18 – 2.12 (br m, 4 H, COD), 1.95 (br m, 2 H, COD), 1.92 (d, 9 H, PCMe_3, $^3J_{PH}$ = 12 Hz), 1.87 (d, 9 H, PCMe_3, $^3J_{PH}$ = 14 Hz), 1.70 – 1.55 (br m, 4 H, COD), 1.57 (s, 3 H, CMe_2), 1.36 (br m, 2 H, COD), 1.29 (s, 3 H, CMe_2), 1.11 (t, 6 H, OCH$_2$CH_3, $^3J_{HH}$ = 7 Hz). ^{13}C{^{1}H} NMR (125.8 MHz, benzene-d_6): δ 153.8 (*C*O), 151.7 (*C*O), 136.7 (*C*H$_{arom}$), 131.6 (*C*H$_{arom}$), 130.8 (*C*CMe$_2$), 130.5 (*C*CMe$_2$), 126.1 (*C*H$_{arom}$), 124.0 (*C*H$_{arom}$), 123.0 (*C*H$_{arom}$), 122.6 (*C*H$_{arom}$), 97.4 (br, COD), 95.8 (br, COD), 72.8 (d, COD, J_{CRh} = 15 Hz), 66.8 (d, COD, J_{CRh} = 15 Hz), 48.5 (NMe_2), 41.6 (N*Me*$_2$), 38.0 (P*C*Me$_3$), 37.2 (P*C*Me$_3$), 35.5 (CMe_2), 34.5 (COD), 34.3 (PCMe_3), 33.8 (COD), 33.5 (PCMe_3), 31.3 (*C*Me$_2$), 29.3 (COD), 28.2 (COD), 27.7 (CMe_2). ^{31}P{^{1}H} NMR (202.5 MHz, benzene-d_6): δ 2.5 (d, 1 P, $^1J_{PRh}$ = 95 Hz), 1.7 (d, 1 P, $^1J_{PRh}$ = 97 Hz). Anal. Calcd for $C_{43}H_{66}Cl_2N_2OP_2Rh_2Zr·OEt_2$: C, 49.91; H, 6.77; N, 2.48. Found: C, 49.48; H, 6.35; N, 2.40. A single crystal of **6·OEt$_2$** suitable for X-ray diffraction analysis was grown from diethyl ether at −30 °C.

Crystallographic Solution, Refinement, and Structural Details for 3·OEt$_2$, 4, and 6·OEt$_2$. Crystallographic data for each of **3·OEt$_2$**, **4**, and **6·OEt$_2$** were obtained at 193(±2) K on a Bruker PLATFORM/SMART 1000 CCD diffractometer using graphite-monochromated Mo Kα (λ = 0.71073 Å) radiation, employing a sample that was mounted in inert oil and transferred to a cold gas stream on the diffractometer. Programs for diffractometer operation, data collection, and data reduction (including SAINT) were supplied by Bruker. Gaussian integration was employed as the absorption correction method for **4**, and the structure was solved by use of direct methods. For each of **3·OEt$_2$** and **6·OEt$_2$**, SADABS (Bruker) was employed as the absorption correction method, and the structures were solved by use of the Patterson search/structure expansion. All structures were refined by use of full-matrix least-squares procedures (on F^2) with R_1 based on $F_o^2 \geq 2\sigma(F_o^2)$ and wR_2 based on $F_o^2 \geq -3\sigma(F_o^2)$. For **3·OEt$_2$** and **6·OEt$_2$**, analogous distances involving the disordered portion of the diethyl ether were constrained to be equal (within 0.001 Å) during refinement. Anisotropic displacement parameters were employed throughout for the nonhydrogen atoms, and all hydrogen atoms were added at calculated positions and refined by use of a riding model employing isotropic displacement parameters based on the isotropic displace-

ment parameter of the attached atom. Additional crystallographic information is provided in the deposited CIF (Supporting Information).

Acknowledgment. We are grateful to the Natural Sciences and Engineering Research Council (NSERC) of Canada (including a Discovery Grant for L.T.), the Canada Foundation for Innovation, the Nova Scotia Research and Innovation Trust Fund, and Dalhousie University for their generous support of this work. We also thank Dr. Michael Lumsden (Atlantic Region Magnetic Resonance Center, Dalhousie) for his assistance in the acquisition of NMR data.

Supporting Information Available: Variable-temperature NMR spectra (PDF) as well as crystallographic data for **3**·$\mathbf{OEt_2}$, **4**, and **6**·$\mathbf{OEt_2}$ (CIF). This material is available free of charge via the Internet at http://pubs.acs.org.

OM700843N